Drug Deliv. and Transl. Res. (2018) 8:150–164
https://doi.org/10.1007/s13346-017-0448-6

REVIEW ARTICLE

Ultrasound-based triggered drug delivery to tumors

Ankit Jain[1] · **Ankita Tiwari**[2] · **Amit Verma**[2] · **Sanjay K. Jain**[2]

Published online: 4 December 2017

Abstract Over the past few decades, applications of ultrasound (US) in drug delivery have been documented widely for local and site-specific release of bioactives in a controlled manner, after acceptable use in mild physical therapy for tendinitis and bursitis, and for high-energy applications in fibroid ablation, cataract removal, bone fracture healing, etc. US is a non-invasive, efficient, targetable and controllable technique. Drug delivery can be enhanced by applying directed US in terms of targeting and intracellular uptake. US cannot only provide local hyperthermia but can also enhance local extravasations and permeability of the cell membrane for delivery of cell-impermeable and poorly permeable drugs. It is also found to increase the anticancer efficacy of drug against solid tumors by facilitating uniform drug delivery throughout the tumor mass. This review summarizes the mechanism of US; various drug delivery systems like microbubbles, liposomes, and micelles; and biological manifestations employed for improving treatment of cancer, i.e., hyperthermia and enhanced extravasation. Safety issues are also discussed for better therapeutic outcomes of US-assisted drug delivery to tumors. This review can be a beneficial asset to the scientists looking at non-invasive techniques (externally guided) for improving the anticancer potential of drug delivery systems.

Keywords Ultrasound · Solid tumor · Cancer · Micelles · Liposomes · Microbubbles

✉ Sanjay K. Jain
drskjainin@yahoo.com

[1] Institute of Pharmaceutical Research, GLA University, NH-2, Mathura-Delhi Road, Mathura, UP 281 406, India

[2] Pharmaceutics Research Projects Laboratory, Department of Pharmaceutical Sciences, Dr. Hari Singh Gour Central University, Sagar, MP 470 003, India

Introduction

Ultrasound is a unique and theranostic modality that can be employed to track drug carriers, trigger drug release, and improve drug deposition with high precision [1]. In the pharmaceutical industries, the application of ultrasound to promote chemical processes is known as sonochemistry. Sonochemistry, or the physical and chemical interactions of ultrasound with molecules, has been meticulously studied [2] and is an essential tool for promoting synthetic reactions used for chemistry as well as for improving drug extraction processes. Ultrasound is being explored for solving issues associated with pharmaceutical manufacturing and formulation, dispersion of solids, and the preparation of colloids. Besides, ultrasound has been employed in the development of nanomaterials, nanocrystals, nanoscale catalysts, etc. Diagnostic imaging is the most important medical application of ultrasound used as a clinical tool, mainly because of its non-ionizing nature and the ability to conduct real-time imaging [3]. Ultrasound energy is used clinically for thermal tissue ablation, hemostasis, and tissue regeneration. Very recent developments have stressed on the use of ultrasound for molecular imaging and ultrasound-mediated therapeutic drug-delivery [4]. Low-intensity ultrasound has been employed in a wide variety of therapeutic applications. Various therapies like sonodynamic, sonoporation, and sonothrombolysis have been used especially for cancer treatment [5]. This review summarizes in a nutshell the mechanism of ultrasound (US); various drug delivery systems such as microbubbles, liposomes, and micelles; and biological manifestations employed for ameliorating the treatment of cancer, i.e., hyperthermia and enhanced extravasation. [6–8]. Safety issues have also been discussed for better therapeutic outcomes of US-assisted drug delivery to tumors. The application potential of US in drug delivery to tumor is represented in Fig. 1.

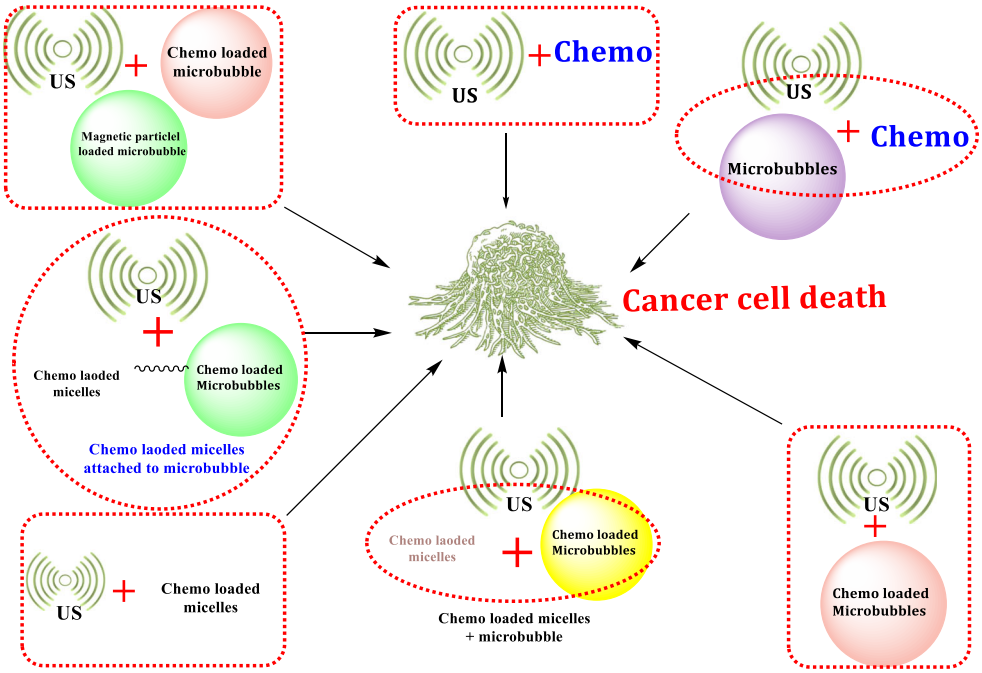

Fig. 1 Application potential of US in drug delivery to tumor

Biological effects of US in therapy: high-intensity focused ultrasound

Biological effects

In the year 1928, the biological effects of ultrasound first appeared when exposure to high-intensity and high-frequency sound waves leading to changes in the living tissues was revealed [9]. The use of focused ultrasound for therapeutic ablation, or ultrasonic surgery, was first proposed in the 1940s [10] and was employed later for the treatment of Parkinson's disease and other neurological conditions. But the therapeutic applications of ultrasound were restricted due to the lack of imaging guidance during the treatment thus lacking safety measures. As the ultrasound imaging progressed to development, various potential hazardous effects of ultrasound were investigated and elucidation of thresholds, damage mechanisms, and propagation properties through tissues was done [11, 12]. The term ultrasonic dosimetry was created to guide the design of ultrasound imaging devices. It relates ultrasound intensity, acoustic pressure, and other physical parameters with the likelihood of producing biological alteration. Ultrasound dosimetry studies meant for the assessment of the safety of diagnostic imaging have led to the advancement in understanding the effects of ultrasound on cells and tissues and, hence, inspired the development of more advanced therapeutics [13]. The propagation of high-intensity acoustic waves through tissues produces two main biological effects: thermal and mechanical. Table 1 gives an overview of the biological effects of US.

Ultrasound in therapy: high-intensity focused ultrasound

Various medical applications of the thermal effects of ultrasound waves gave rise to high-intensity focused ultrasound, widely known as HIFU. Although the maximum permitted time-averaged intensity of diagnostic ultrasound is 0.72 W/cm^2, HIFU has intensities in the range of 100 to 10,000 W/cm^2 [28]. The ultrasound wave is brought into a focus usually 1 mm in diameter and 10 mm in depth such that the thermal effects are localized. The temperature rises at the focus to higher than 60 °C for several seconds causing irreversible cell death. Because of the ability of HIFU to focus high-intensity waves which makes it a non-invasive treatment option for ultrasound surgery, frequencies as low as 500 kHz are used for skull treatment or deep tissue treatments whereas frequencies as high as 8 MHz have been used for superficial therapies such as intraurethral prostate treatment [29]. In the early 1980s, HIFU was used for treating glaucoma and intraocular tumors but was finally replaced by laser technology. However, there is renewed interest in HIFU for ophthalmological applications due to better focusing capabilities. By the mid-1980s, multiple groups were engaged in HIFU for the treatment of tumors by inducing either localized hyperthermia or tissue ablation leading to multiple clinical trials. Recently, various clinical applications of therapeutic HIFU have expanded to include treatment of tumors of the prostate, the breast, the heart, the pancreas, the liver, and the esophagus [30, 31]. HIFU has also been suggested for the treatment of thrombolysis, hemostasis, and venous insufficiency. Researches

Table 1 An overview of the biological effects of US

Type of effect	Phenomena involved	Phenomenal changes	Uses	Ref.
Thermal	Attenuation	Increase in the tissue temperature due to US	Designing and planning of thermal treatment of the bone, the prostate, the heart, and the brain	[14–22]
Mechanical	Acoustic cavitation, microstreaming, and radiation force	Elevation in temperature and pressure with emission of light	Various therapeutic applications involving mechanical bioeffects	[23–27]

evaluating the pathological changes in normal and malignant human tissues following exposure to HIFU have demonstrated that thermally ablated tissues undergo homogeneous necrosis with irreversible tumor cell death and severe damage to tumor blood vessels. HIFU has also been found to initiate acute inflammatory responses increasing tumor tissue destruction via immune cell activation, which could synergistically enhance the treatment response with other therapies [32]. Currently, three main categories of HIFU devices are used in the clinical setting and are usually classified on the basis of the ultrasound energy delivery path: (a) extracorporeal, (b) intracavitary, or (c) interstitial. Extracorporeal devices are generally used for targeting readily accessible organs through an acoustic window on the skin such as uterine fibroids or the breast [33], intracavitary devices are employed for transrectal and transurethral prostate cancer treatments or for intraesophageal treatment, and interstitial devices are used for treating the targets which are difficult to access, e.g., the biliary duct. The FDA approved a HIFU device in October 2004 for the treatment of uterine fibroids, ExAblate (Insightec, Haifa, Israel), which uses magnetic resonance imaging (MRI) for treatment guidance and monitoring. Recently, the FDA classified HIFU systems as class II (special controls) devices, to provide a reasonable assurance of safety and effectiveness of the equipment [34, 35]. Advanced devices such as Sonalleve (Phillips, The Netherlands) and ExAblate 2100 (Insightec, Haifa, Israel) are currently approved for clinical use in uterine fibroids and in bone metastases for the relief of pain [36].

Methods of applying HIFU for non-invasive tumor drug delivery

Elevated response to therapeutic agents after exposure to ultrasound has evoked attention in HIFU as a drug delivery tool [37]. The mechanisms which are considered to be responsible for ultrasound-mediated drug delivery are acoustic cavitation and the associated microstreaming effects from localized forces. Despite the similarity in the physical mechanisms behind the enhanced delivery, applications have been divided on the basis of their therapeutic goal. The mechanism of acoustic cavitation and the types of cavitation are shown in Fig. 2.

Sonophoresis

The first report of transdermal enhanced delivery of drugs using ultrasound was found in the year 1954 in which hydrocortisone was used for the treatment of polyarthritis in conjunction with ultrasound. This delivery method is called as sonophoresis and is presently employed as a powerful tool to enhance transdermal drug delivery and achieve non-invasive drug administration [38]. The technique utilizes shock waves generated from collapsing cavitating bubbles found in the skin, which introduce minute openings in the intracellular spaces permitting the passage of small molecules. Sonophoresis is usually performed by devices that work under 100 kHz because cavitation is more common at lower frequencies. Since HIFU is normally performed at higher frequencies and depths, it is not associated with sonophoresis. However, the energy levels necessary for sonophoresis as well as the reported bioeffects are quite compatible with HIFU devices. Sonophoresis facilitates the delivery via inducing the dispersion of the drug throughout the epithelial layers, but no evidence has been given for the enhancement of intracellular delivery [39].

Sonoporation

The phenomenon of transient permeabilization of cell membranes via ultrasound-induced pores in the lipid bilayer is referred as sonoporation. The induction of inertial cavitation at an interface like the membrane of a cell or a tissue barrier by ultrasound causes microbubbles within the focal point to collapse in a non-spherical manner driving high-speed jets of liquid into the interface. These jets are supposed to produce temporary pores in the cell membrane as well as lead to microstreaming in the extracellular environment. The therapeutic agents pass through the pores propelled in part by the mechanical effects of microstreaming with additional effects from ultrasound-induced endocytosis [40]. Cavitation can be attained by two ways: (i) natural formation of microbubbles under the influence of the high-intensity ultrasound waves or (ii) by exogenous systemic administration of microbubbles. Microbubbles employed for sonoporation are clinically approved diagnostic ultrasound contrast agents [41] and are available in either microcrystalline or microbubble emulsion

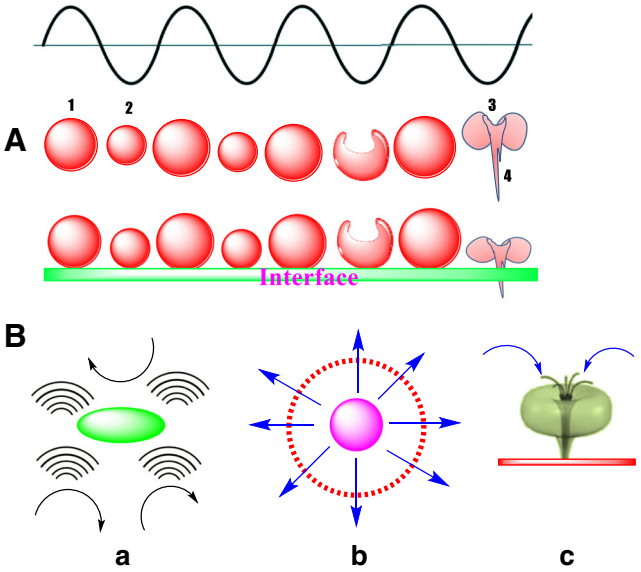

Fig. 2 Mechanism of acoustic cavitation and types of cavitation. Pressure change in the propagation medium is generated by ultrasound waves in the presence of microbubbles. Microbubbles may be either **a** floating in the medium or **b** pushed via radiant force against the medium. In the presence of external cavitation the microbubbles (1) expand and contract, (2) explode due to pressure changes, (3) and lead to liquid streaming or jetting. (4) The generation of force by the high-pressure jet may lead to the formation of pores in the cellular membrane [(a) stable cavitation, (b) inertial cavitation, and (c) asymmetrical cavitation]

forms. Recently, tracking of perfluorocarbon nanoemulsion delivery as a new technique has been reported using fluorine-19 MRI for precise HIFU tumor ablation [42]. Table 2 depicts various currently available ultrasound contrast agents used for sonoporation along with their compositions. Figure 3 represents microbubbles as delivery agents.

Ultrasound has been successfully employed in preclinical studies for introducing membrane-impermeable agents into cells or tissues like small interfering ribonucleic acid (siRNA), peptides, nanoparticles, and antibodies [43, 44]. The application of sonoporation for the treatment of cancer [45], cardiovascular disease, and gene therapy [46] is currently being explored. Besides the therapeutic effect caused by enhanced drug delivery into the cells, sonoporation has also been evinced to enhance the cytotoxicity of anticancer therapeutic compounds and stimulate ultrasound-induced apoptosis. Ultrasound-induced apoptosis is noticed as a delayed biological effect in tissues exposed to high-intensity ultrasound, especially in cells with poor regeneration, e.g., neurons. Efforts to ameliorate sonoporation-based therapies have led to the development of microbubbles (chemically modified) that either possess receptor-targeting ligands or carry a drug payload. Certain advanced microbubbles that target a specific cell receptor have been designed for ultrasound imaging and include microbubbles that bind to the *P*-selectin of activated platelets for atherosclerotic plaque detection [47].

Blood–brain barrier disruption

Various other uses of ultrasound cavitation have been explored such as the treatment of gliomas through locally induced transient disruption of the blood–brain barrier (BBB) produced by employing a combination of high-intensity ultrasound, doxorubicin (Dox), and Optison® microbubbles [48–50]. Similar to sonoporation, cavitation is also considered to be the main mechanism behind the reversible opening of the BBB improving drug uptake in the brain. Initial work disclosed that short, high-intensity ultrasound waves above the cavitation threshold produced temporary disruption of BBB. Unfortunately, brain tissue damage in certain animals hindered the therapeutic benefit. It was sorted when BBB disruption was consistently produced using focused ultrasound with concomitant injection of intravascular gas microbubbles as supplementary cavitation sites. Moreover, the use of microbubbles decreased the necessary ultrasound intensity to levels below the threshold fostering thermal damage to adjacent brain tissue [51]. The physical mechanism for BBB disruption is ascribed to microbubble cavitation activity, but the bioeffects are different in comparison to sonoporation. The passage of microbubbles through the tissue exposed to ultrasound causes their expansion and contraction at the frequency of the propagating acoustic wave because of the cyclic pressure reductions generating mechanical forces and microstreaming. In addition, a radiation force pushes the bubbles towards the vessel wall. Above an intensity threshold, the bubbles collapse near the vessel wall producing fluid jets that can puncture the BBB permitting the passage of molecules through the barrier. Various studies regarding the cellular mechanisms of this disruption have revealed that macromolecule permeability is due to the mechanical forces stimulating

Table 2 Various currently available ultrasound contrast agents used for sonoporation along with their compositions

Contrast agent	Composition
Albunex	Air-filled albumin microspheres suspended in 5% *w*/*v* human serum albumin
Optison	Perflutren protein type A microspheres (human serum albumin) and perflutren (octafluoropropane gas)
Echovist-200	Microcrystalline suspension of galactose
Levovist	Microcrystalline suspension of galactose and palmitic acid in sterile water

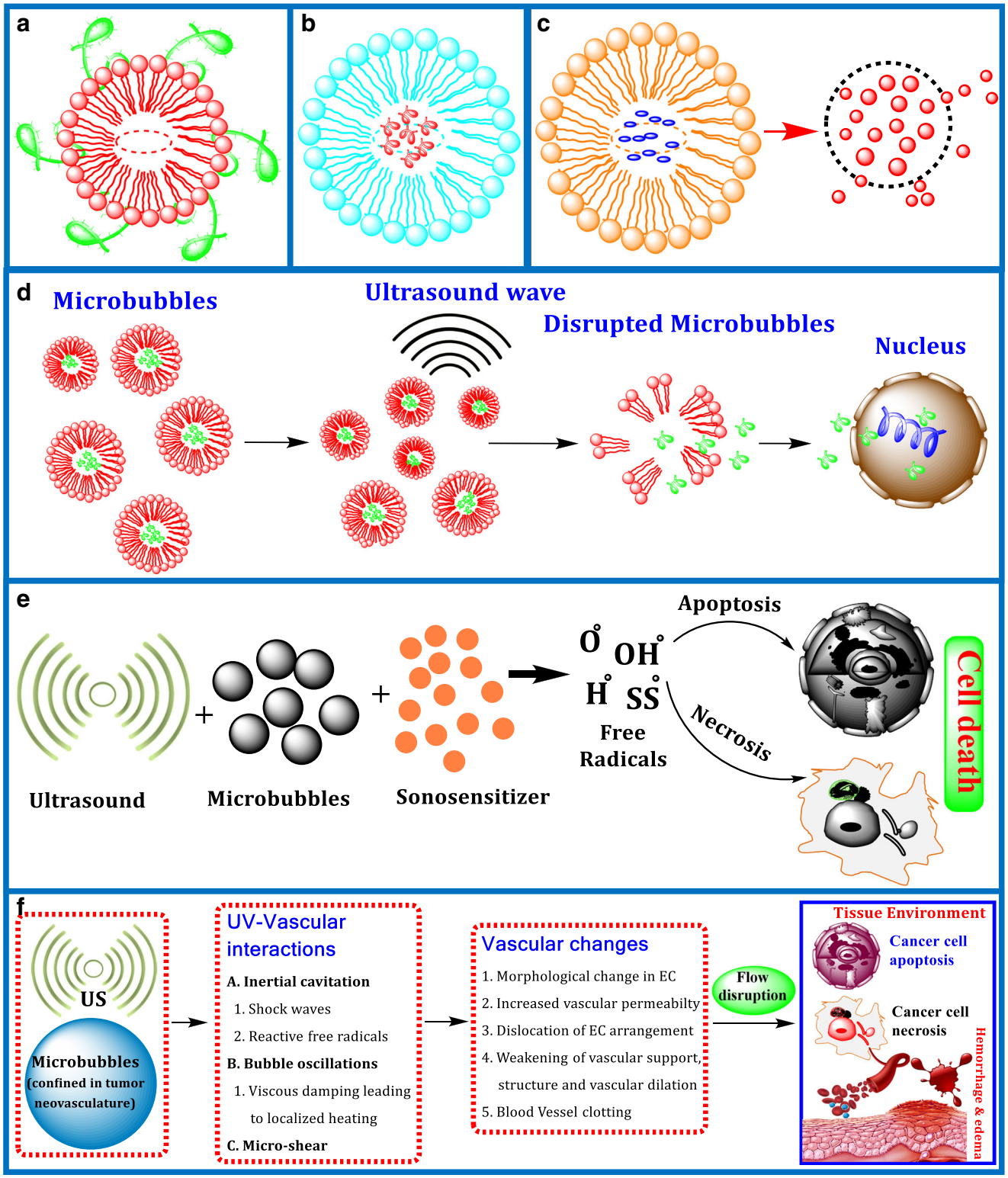

Fig. 3 Microbubbles as delivery agents. Attaching ligands on the hydrophobic ends may form gas microbubbles as delivery agents. **a** Ligands encapsulated within the microbubble would get delivered by its collapse. **b** Drugs/nanoparticles encapsulated would be delivered by the collapse of the microbubbles. **c** These microbubbles act as a drug carrier or are used in gene therapy etc. **d** Sonoporation-based delivery using mircobubbles. **e**, **f** Sonoporation-based cancer therapy using mircobubbles

the formation of channels and fenestrations in the endothelial cell wall, the widening of interendothelial clefts, and the high pressures which cause easy movement through the injured endothelial lining [52]. When employing microbubbles in

combination with ultrasound, the BBB disruption has been manifested to be reversible with the least damage to the tissues in vicinity in the case of animals. Magnetic resonance imaging demonstrated that the BBB showed increased permeability up to 24 h after ultrasound exposure with optimal uptake in the brain in 6 h. The safety investigations of BBB disruption revealed that permeability is induced at 690 kHz, and a pressure value of 0.4 MPa significantly below 2.3 MPa is needed for tissue necrosis [53]. Histological analysis of adjacent tissues after BBB disruption revealed insubstantial levels of apoptosis or ischemia, with no major differences up to 4 weeks after the disruption. Various animal models such as rabbits, rats, and mice have been used to validate ultrasound-mediated BBB disruption. HIFU successfully delivered dopamine receptor antibodies, enhanced the response of brain cancers to Dox and trastuzumab, and promoted the uptake of therapeutic antibodies for Alzheimer's treatment and DNA for gene therapy [54]. Park et al. (2017) employed dynamic contrast-enhanced magnetic resonance imaging (DCE-MRI) for characterizing focused ultrasound (FUS)-induced permeability changes which were stimulated by FUS in a rat glioma model as well as in the normal brain and to understand the relation between these alterations and the resulting concentration of Dox. Through this investigation, it was evinced that FUS and microbubbles, apart from increasing Dox delivery across the BBB and the blood–tumor barrier (BTB),were retained in the tissue at considerably raised levels for a minimum period of 24 h. It is suggested that increased retention may enhance the potency of doxorubicin and reduce the dose [55]. Recently, Airan et al. exploited small-molecule anesthetic propofol using focused US and nanoparticles for transcranial drug delivery as promising non-invasive, focal, and image-guided clinical neuromodulation technique [56]. Novel formulations for microbubbles that target the BBB may significantly enhance barrier permeability and have vast potential for the introduction of proteins and other impermeable agents of therapeutic significance into the brain. Figure 3 depicts the application of microbubbles as delivery agents.

Hyperthermia-triggered drug delivery

Hyperthermia-triggered drug delivery is defined as the release of a drug at the desired site of action induced by the thermal effects of HIFU. This technique is aimed at increasing the therapeutic index of chemotherapeutics, which often leads to side effects due to their distribution into normal healthy organs and tissues [57, 58]. Temperature-sensitive liposomes (TSLs) have been developed in order to improve drug toxicity profiles while simultaneously protecting the drug from rapid metabolism and excretion [59, 60]. TSLs encapsulate a hydrophilic drug within a core surrounded by a lipid bilayer. Enhanced retention and permeability effect of nano-sized liposome drug leads to the passive accumulation of the TSL into tumors. The rapid and complete release of the drug into the tumor region by mild hyperthermia leads to site-specific drug delivery. Mild hyperthermia of the tumor area and local vasculature is usually induced by micro-, radio-, or ultrasound waves [61]. Although the spontaneous accumulation of drug containing liposomes typically occurs in tumor xenografts, mild local hyperthermia significantly enhances drug delivery into cancer cells and its therapeutic response. Additional advantages from local hyperthermia result from enhancing the accumulation of the TSL in the tumor tissue. In addition, elevated blood flow to the tumor area along with enhanced cell permeability from hyperthermia stimulates improved delivery into the cells of the tumor. The successful preclinical studies have led to a series of clinical trials evaluating a Dox-loaded TSL called ThermoDox® (Celsion) for the treatment of hepatocellular carcinoma (phase III) and invasive breast cancer (phase I) using microwaves to induce hyperthermia. The precision and clinical application of TSL-based chemotherapies could be improved by the use of HIFU to induce mild heating deep into the tissues. Various advantages of HIFU are the ability to focus and control heating by scrupulous choice of the acoustic parameters like continuous or pulsed wave energy, frequency, and intensity. Another significant benefit of using HIFU for hyperthermic drug delivery is its compatibility with MRI which permits real-time thermometry monitoring of tissue temperature. Recent efforts to use MR-guided HIFU to deliver ThermoDox were examined in rabbit muscle revealing higher Dox uptake in the area of hyperthermia [62]. ThermoDox with HIFU was assessed as a complementary therapy to the thermal ablation of bone cancer with better results. The application of molecular imaging to visualize and quantify HIFU-induced TSL drug release has recently grabbed attention. For example, TSL co-encapsulated with a gadolinium contrast agent and Dox enabled the imaging of TSL content release as described in vitro using squamous carcinoma cells and later in a tumor. For translating HIFU into a drug delivery method for use in the cancer clinic, certain improvements are to be made. HIFU is a suitable preclinical tool for investigating the suitability of new formulations and compositions of TSL as well as for the evaluation of new ultrasound-sensitive drug carrier nanoparticles. For example, PEG polymer-modified advanced nanosized "stealth" TSLs are exhibiting high Dox loading capacity, enhanced physiological stability in circulation, faster drug release upon mild HIFU heating, and enhanced efficacy as compared to the traditional lysolipid TSL [63]. Recently, efforts have been made for the expansion of the use of nanoparticles for encapsulating hydrophobic drugs using ultrasound-sensitive micelles composed of hydrophobic polymers [57, 64–66]. MR-guided high-intensity focused ultrasound (MR-HIFU) permits the application of hyperthermia in a non-invasive, localized, and controlled manner. Recently, several preclinical studies reported HIFU-induced drug delivery in various animals like mice, rats, and rabbits

[67]. MR-based temperature mapping has been developed for MR-guided HIFU ablation procedures providing near-real-time temperature readings of the targeted tissue. Recently, various hyperthermia-induced drug delivery studies using MR-HIFU have been demonstrated. A clinical MR-HIFU system was employed with a 256-element high-intensity focused phased-array ultrasound transducer integrated into the patient's bed MRI [68]. The system was extended with a dedicated small-animal MRI coil that fits onto the ultrasound transducer. Since the MR-HIFU permitted volumetric beam steering, whole rat tumor could be covered in one treatment. MR-based temperature maps served as an input for a binary feedback control algorithm to the ultrasound transducer for maintaining mild hyperthermia over 30 min with interleaved T1 mapping of the tumor tissue to follow the release of the MRI contrast agents from its liposomal carrier. Dox-containing TSLs were injected at a dose of 5 mg Dox/kg, and experiments were performed without HIFU but with HIFU-mediated hyperthermia. The MR images depicted a decrease in T1 across the tumor in HIFU-treated tumors revealing the release of the MRI contrast agent from the TSL, while in non-heated tumors, T1 decreased only marginally using the paramagnetic TSLs. The variation in longitudinal relaxation rates ($\Delta R1 = \Delta 1/T1$) demonstrated a good correlation with the amount of Dox in the tumor as evinced from ICP-MS and HPLC, respectively. A significant change was visible in rat 2, of T1 in the tumor rim, whereas the center of the tumor showed no change. In adjacent histological studies, few tumors seemed to have a poorly perfused necrotic core and a well-vascularized tumor rim, which might be the reason for the lack of contrast agent delivery in the tumor core as visualized in the MR images of rat 2 [35]. In another study, hyperthermia either as alone treatment or before ablation rendered homogeneous TSL, [$Gd(HPDO_3A)(H_2O)$], and Dox deliveries across the tumor. The combination of hyperthermia-triggered drug delivery followed by ablation exhibited better therapeutic results as compared to other treatments owing to direct induction of thermal necrosis in the core of the tumor and efficient drug delivery to the tumor site [69]. Staruch et al. demonstrated a temperature-induced drug delivery of Dox employing ThermoDox® and a focused US transducer which was scanned to cover the entire tumor [62]. The MRI provided temperature maps as a feedback for power control to maintain a target temperature of 43 ± 1 °C for a time span of 25 min. For their research, New Zealand rabbits were prescribed Dox at a dose of 2.5 mg/kg. On an average, a 17-fold rise of Dox was observed in heated muscle tissue compared with non-heated muscle tissue. Dai et al. developed and characterized thermo-responsive magnetic liposomes, by combinining characteristics of magnetic targeting and thermo-responsive control release for hyperthermia-triggered local drug delivery. MagABC liposomes, when targeted to tumor cells in culture by a permanent magnetic field, yielded a significant enhancement in intracellular accumulation of Dox in comparison to non-magnetic ammonium bicarbonate (ABC) liposomes. This led to an enhancement in cytotoxicity for Dox-loaded MagABC liposomes in comparison to Dox-loaded ABC liposomes in tumor cells [70]. In another study, low-intensity US-controlled delivery of Dox was reported for local cytotoxicity and drug release via induced destruction and degradation of microparticles of poly(lactic-co-glycolic acid) (PLGA). US-triggered MP destruction/degradation remarkably increased cell death and drug release [71]. US-induced mild hyperthermia (41–43 °C) has been found to improve the anticancer efficacy of both Taxol®- and paclitaxel-loaded nanocapsules. Boissenota et al. studied the influence of ultrasound on paclitaxel-loaded nanocapsules in vitro and in vivo. These nanocapsules had a shell of PLGA-PEG and a liquid core of perfluorooctyl bromide (PFOB). In in vivo studies in a subcutaneous CT-26 colon cancer murine model, there was increased inhibition of tumor growth for both paclitaxel-loaded nanocapsules and Taxol® under hyperthermia conditions owing to the enhancement of local cytotoxic efficacy [72]. Recently, nanoscale bubble-generating liposomes (liposomes containing ammonium bicarbonate) have been developed. These liposomes showed increased localization in the tumor interstitial space owing to the EPR effect, but synergized with HIFU ablation, the lipsomes improved the survival of breast tumor-bearing BALB/c nude mice [73]. A bubble-generating liposomal delivery system has been developed by introducing ammonium bicarbonate and gold nanorods into folic acid-conjugated liposomes for simultaneous multimodal imaging and the local release of Dox with hyperthermia. Ammonium bicarbonate controlled the rapid release of drug in the tumor microenvironment, and ultrasonic cavitation enhanced the therapeutic efficiency to a great extent [74]. Santos et al. combined focused US with two-photon microscopy for hyperthermia-mediated Dox delivery using thermosensitive liposomes and in vivo real-time imaging, respectively. It was found that there was abrupt release of Dox within 30 s at 42 °C [75]. Figure 4 shows the release of the payload from thermosensitive liposomes with Tc around 42 °C at mild elevated temperature. Figure 5 represents US-mediated intracellular drug delivery utilizing temperature-sensitive liposomes (step 1) and membrane permeabilization in the presence of microbubbles (step 2).

Sonodynamic therapy

Umemura and scholars evoked sonodynamic therapy (SDT) for the first time [76]. It is a novel treatment in which photodynamic therapy (PDT) formed the base for its development. Both the therapies have a resembling mechanism of tissue penetration. After the absorption of the sound sensitizer, the target tissues would be irradiated by SDT with the help of ultrasonic waves, which leads to the retention of the sound

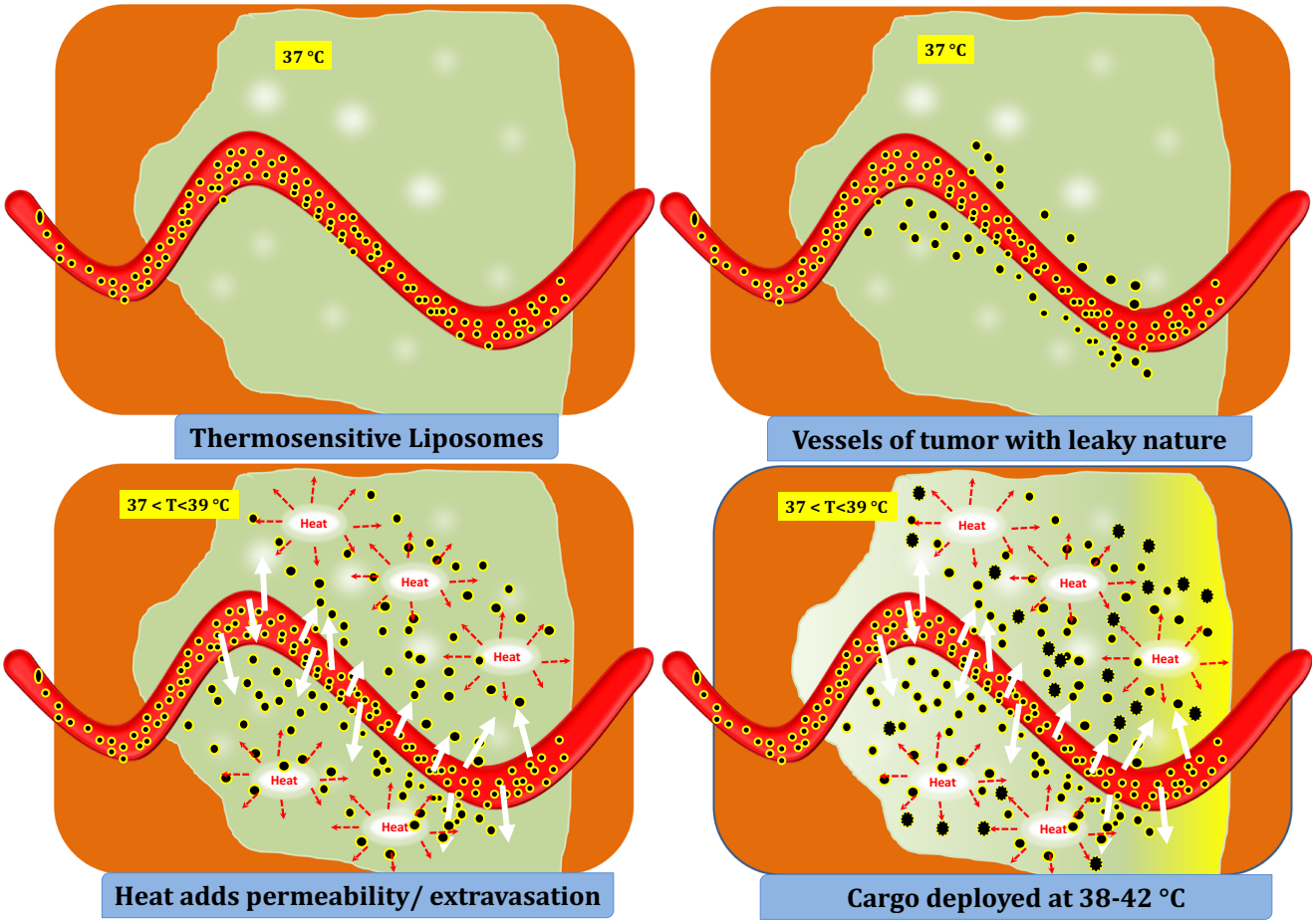

Fig. 4 Thermosensitive liposomes with Tc around 42 °C releasing the payload at mild elevated temperature

sensitizer inside the target cell for obtaining energy and producing electron transitions. The reactive oxygen species (ROS) is generated when the electron returns to normal state from the transition state [77]. The research, which has been conducted in 20 years, has led to the discovery that SDT has the ability to treat solid tumor, gliomas, leukemia, oral squamous cell carcinoma, atherosclerosis, etc. SDT, as a new non-invasive treatment developed from PDT, can kill tumor cells

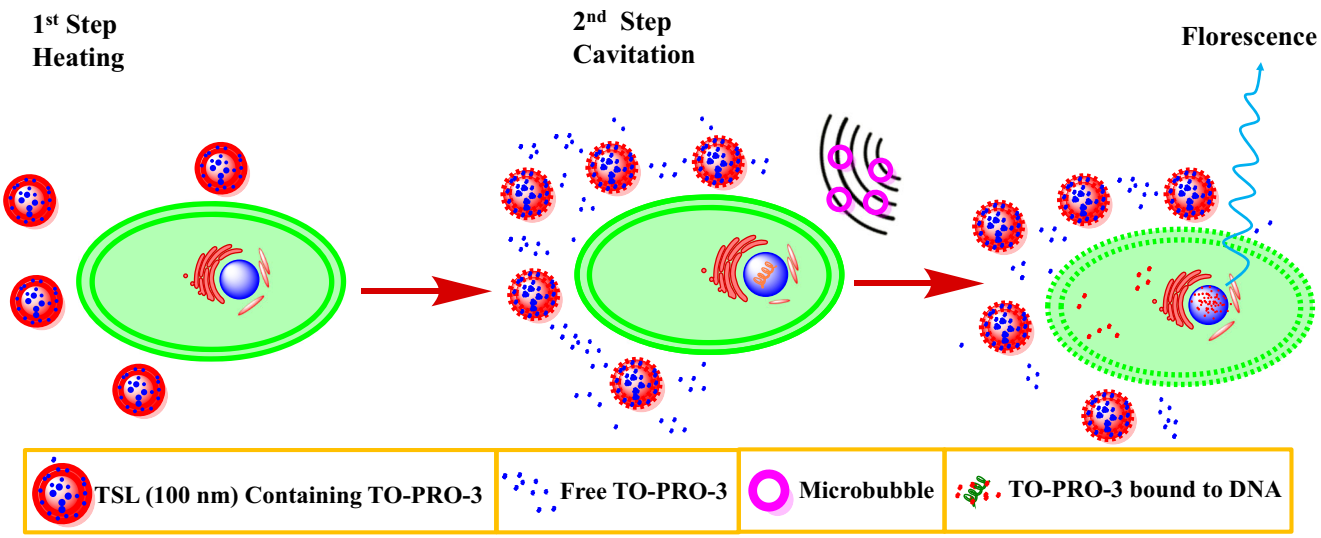

Fig. 5 Schematic representation of US-mediated intracellular drug delivery utilizing temperature-sensitive liposomes (step 1) and membrane permeabilization in the presence of microbubbles (step 2)

specifically and selectively. Due to the novel application aspects of SDT, it has gained more attention from numerous researchers in recent years and is being explored by the scientists [78]. There are various advantages of SDT as follows: (a) non-invasive treatment: minimum necessity of invasive guidance, for example, endoscopic punctured optical fiber in SDT treatment; (b) good repeatability: SDT has the ability of treating the deep tumor for various times; (c) deep penetrability: ultrasound has the capability to penetrate into deeper tissues (tens of centimeters) and permits the SDT to treat deep human tumors without the need of CT/MRI or endoscope [79]; and (d) lower cost: CT/MRI is not required by SDT therefore making it quite easy for clinical expansion.

Sonosensitizers

Majority of the sensitizers which were earlier employed in SDT-based studies were porphyrin-based molecules that had been utilized as photosensitizers, and examples are hematoporphyrin and Photofrin®, a commercially available hematoporphyrin derivative that is used extensively in clinical PDT. The previous researches, depicting sonodynamic effects, apparently reported that ROS was produced by the porphryin-based sensitizers on exposure to ultrasound, and it was proposed that ultrasound-responsive cytotoxicity was induced by the ROS in a similar way as in PDT. Indeed, it was manifested in a study that employing similar acoustic field properties, protoporphryin IX seemed to be more active as a sonosensitizing agent as compared to hematoporphyrin, while later studies demonstrated that it was because of the observation that cells had taken more protoporphryin IX [80, 81]. Though porphyrins had been exhibited to be capable of sonodynamic effects, it was identified that these are comparatively hydrophobic and despite being taken up by tumor cells to some extent, they depicted a ubiquitous distribution in other tissues. Although it is quite effective as a sonosensitizer in vitro, its utility is contraindicated in vivo due to the rapid sequestration in the liver and concomitant clearance [82]. Mitochondrion-targeted liposomes loaded with sonosensitizer for SDT of caner have been reported recently. The (3-carboxypropyl) triphenylphosphonium bromide (TPP) was grafted onto the liposomes using cholesterol (Chol) as linker for mitochondrion targeting. The hematoporphyrin monomethyl ether (HMME) was encapsulated within the liposomes, and its release was triggered by the irradiation of an extra ultrasound owing to the oxidation of the lipid in liposomes. These liposomes showed enhanced accumulation in the mitochondria and increased cancer cell death by HMME under SDT [83]. A few examples of sonosensitizers are as follows [84, 85]:

- Acridine orange is a sonosensitizer which generates O_2+ OH as ROS at an ultrasound frequency of 2 MHz.
- Chlorin-e6 is a sonosensitizer which generates O_2+ ROO as ROS at an ultrasound frequency of 1.56 MHz.
- Photofrin is a sonosensitizer which generates O_2 as ROS at an ultrasound frequency of 1 MHz.
- DCPH-P-Na(I) is a sonosensitizer which generates O_2 as ROS at an ultrasound frequency of 1 MHz.
- Hematoporphyrin is a sonosensitizer which generates O_2 as ROS at an ultrasound frequency of 1.92 MHz.

Therapeutic mechanisms

There is a distinct association between ultrasound exposure, the presence of the sonosensitizer, and the production of ROS, and it has been found that the cytotoxicity is evoked by the ROS production.

Ultrasound-mediated ROS generation As ultrasound traverses via a liquid/tissue, oscillation of microbubbles present in the liquid takes place in the enforced acoustic field. As the acoustic pressure increases, the stability of the oscillation decreases and finally the implosion of the bubble occurs. Due to the presence of very high temperatures and pressures at the point of implosion, release of energy in the form of heat and light takes place. Due to the presence of extremes in pressure and temperature, the imploding bubble might be considered as a sonochemical reactor. Numerous previous studies related to recognition of various cytotoxic ROS formed during the sonodynamic induction of porphyrins were performed with few free radicals like histidine and mannitol.

The sonodynamic and photodynamic effects on free radical production and cell cytoxicity were compared with various photosensitizers by Hiraoka et al. [86]. Ultrasound at a frequency of 1.2 MHz and intensities from 0.5 to 3.1 W/cm^2 were employed in this analysis, when hematoporphyrin was allowed to be exposed to light, and production of TAN (2,2,6,6-tetramethyl-4-piperidione-*N*-oxyl)was observed, depicting that the production of singlet oxygen took place during stimulation.

The function of sonoluminescence Sonoluminescence refers to the emission of light from cavitating bubbles, and despite a lack of knowledge and uncertainty of the exact mechanism, it has been proposed that it may ensue from blackbody radiation, recombination radiation, or combinations of any of these. Umemura et al. evidenced the emission of light from saline solutions employing ultrasound conditions which were used to arouse sonodynamic effects. A peak in the range of 400–450 nm was depicted by the spectrum line (SL) light emission, and it was manifested that the SL emissions were absorbed by hematoporphyrin absorbed. The authors concluded that hematoporphyrin being a photosensitizer can be activated by the SL

light. This could explicate the production of singlet oxygen species during the sonodynamic activation [76].

Sensitizer-dependent destabilization of cell membranes It is already an established fact that porphyrins undergo an interaction with cell membranes, and it has been described by Stepniewski et al. [87]. There might be an interaction between the cell membrane and the hydrophobic entity which might depict that the cell membrane may be hypersensitive to ultrasound; few studies demonstrate that the membrane lipids get chemically modified when exposed to ultrasound in the presence of a sensitizer [88]. In this study, the authors evidenced that treating the cells with hematoporphyrin and ultrasound led to a reduction in the membrane fluidity due to the lipid peroxidation. This reduced membrane fluidity led to a reduction in the activities of adenylate and guanylate cyclase.

Applications in cancer treatment

Though recent research on SDT treatment has proven its effectiveness in killing many solid tumors, only a few experiments reach the animal and clinical trial stages [89].

The various applications of SDT include

- treatment of gliomas [90],
- breast tumor [91],
- prevention of atherosis [92],
- treatment of periodontitis,
- ability to kill pathogenic microorganism [93], and
- elimination of proliferative cicatricose [94].

Application of US for triggered drug delivery to tumor

Since a couple of years ago, ultrasound has been applied for various therapeutic purposes in the field of medicine. Applications of ultrasonic energy have been continuously expanding in transdermal drug delivery, fracture healing, cataract removal, etc. Therapies are associated with few undesirable effects like burns and hemorrhage. For achieving an optimal benefit-to-risk ratio, side effects must be minimized and proper standardization ought to be done when therapeutic applications of ultrasound are taken into consideration. Continuous efforts in the field of ultrasound may discover some novel treatments. Table 3 summarizes the biophysical basis for therapeutic applications based on heating, non-thermal mechanisms, and multiple mechanisms.

Table 3 The biophysical basis for therapeutic US applications

Based on heating					
Therapeutic applications of US	Trigger used	Frequency used (MHz)	Application	Ref.	
Physical therapy	Handheld transducer	–	In sports medicine	[95]	
Hyperthermia	Multielement applicators	1–3.4	Cancer therapy	[96]	
High-intensity focused ultrasound	Focusing transducer	0.5–7	Uterine fibroids, cardiac ablation, and various esthetic treatment	[33, 97]	
Based on non-thermal mechanisms					
Therapeutic applications of US	Probes used	Frequency used	Applications	Associated risks	Ref.
Extracorporeal shock wave lithotripsy	Piezoceramic	150 kHz	Orthopedic indications such as plantar fasciitis and epicondylitis	A high systemic blood pressure, reduced renal function, onset of hypertension, an increased incidence of stone recurrence	[98, 99]
Intracorporeal lithotripsy	Electrohydraulic probes	Up to 1000 kHz	Treatment of stones	Hemorrhage, ureteral perforation, urinary tract trauma, and infection	[100, 101]
Kilohertz-frequency US devices	Ultrasound probe	20–90 kHz	Advanced surgical procedures for tissue cutting, hemostasis, and tissue removal	Bleeding, scarring, and infection	[102]
Based on multiple mechanisms					
Therapeutic applications of US		Frequency	Applications		Ref.
Catheter-based US		2.2 MHz	Thrombolysis		[103]
Skin permeabilization		< 100 kHz	For delivering heparin or insulin via the skin		[104]
Low-intensity pulsed ultrasound		1.5 MHz	Non-healing fractures		[105]

Recent advances

A sound-excitable drug (SED) that is non-cytotoxic to cells has been developed recently to disrupt the plasma membrane under mild ultrasound insonation, i.e., 1 MHz at 1 W/cm^2, with utmost safety. SEDs insert into the plasma membrane and weaken the membrane's integrity, and US energy destabilizes the SED-disrupted membranes in insonation that leads to membrane rupture and ultimately cell death [106]. In a recent study, Staruch et al. utilized the same system with comparable experimental parameters for the temperature-induced delivery of drug at the bone/muscle tissue interface. The muscle tissue adjacent to the thigh bone was heated up to a temperature of 43 °C. On the basis of the distance between the control planes to the bone/tissue interface, the temperatures obtained at the bone/tissue interface and within the bone were estimated to vary between 46 to 78 °C. Dox extractions from the tissues depicted ten times the enhancement in heated bone marrow and approximately 16 times the enhancement in heated muscle tissue [107]. Kong et al. reported quantitative modeling of the pharmacokinetics of Dox and Dox release from TSLs. In the first analysis, the drug concentration in the tumor scales with the time span of hyperthermia, the plasma concentration of TSL, the drug payload per TSL, and the perfusion of the tumor tissue were approximated. As the TSLs stay predominantly in the blood stream because of their size (100–200 nm), the drug will be intravascularly released within the heated tumor (41–42 °C) thereby creating a concentration gradient which drives tumor uptake [108]. The subsequent drug uptake in the tumor is governed by its pharmacokinetic and pharmacodynamic properties and perfusion of the tumor as well. With an increase in the tumor perfusion, the drug concentration in the tumor tissue also increases until a maximum is reached, where drug uptake into the tumor becomes the rate-limiting step. In order to compete against downstream washout, the uptake and retention of the drug in the tumor tissue need to be significant. Higher perfusion can also lead to a decrease in uptake, when downstream washout is faster than drug uptake in the tumor or when the transition time through the tumor is faster than the time required to achieve release from TSLs [109]. For drugs with a high free volume of distribution, hyperthermia should be applied first and maintained while injecting TSLs. Hyperthermia time span should be reasonably long; however, further drug accumulation in the tumor levels off due to a lowering in the plasma level of the drug. The clearance of TSLs and drugs depends on species and scales inversely with cardiac output. For clinical application, hyperthermia for 30–60 min after injection of the TSLs appears a good compromise between achievable drug levels, technological issues to maintain controlled hyperthermia, and patient comfort. A different protocol should be considered for the TSL-containing drugs that have rapid washout since they are not adequately retained in the tumor tissue upon vascular release. Firstly, temperature-sensitive drug carriers are injected and are taken up by the lesion via the enhanced permeability and retention effect often observed in tumor tissues [110]. The drug is rendered bioavailable after the drug carrier system received sufficient tumor accumulation. This protocol could exert a significant role for liposomal drug formulations with low efficacy in clinical trials because of stable encapsulation of the drug in the liposomes as seen in the case of liposomal cisPt formulations [111]. Yudina et al. considered a two-step delivery approach for cell-impermeable drugs with an intracellular target. In this study, temperature-mediated drug delivery was combined with pressure-mediated drug delivery using TSL containing a cell-impermeable (model) drug. Once adequate accumulation of the TSL at the diseased site is reached, temperature-triggered drug release could be induced, while a subsequent mechanical trigger via US in the presence of microbubbles is employed to enhance the permeability of the cell membrane to mediate drug uptake into the cytosol [112]. Chemical gas (CO_2)-generating carbonate co-polymer nanoparticles (Gas-NPs) have been developed to improve in vivo performance of nanocarriers with higher tumor targeting ability in addition to the high quality of echo properties for tumor-targeted US imaging. These nanoparticles when loaded with anticancer drug showed desirable theranostic functions for US-triggered drug delivery after i.v. injection into tumor-bearing mice [113]. Cell-penetrating peptide Dox conjugate-loaded asparagine–glycine–arginine (NGR)-modified nanobubbles have been developed for US-triggered drug delivery. There was increased cell uptake in human fibrosarcoma cells (HT-1080, CD13+) under US effect as compared to the treatment without US. In vivo studies in nude mice xenograft of HT-1080 cells showed higher tumor inhibition effect and improved median survival time and safety than treatment with the normal Dox injection group and without US effect [114]. In a similar approach, peptide–camptothecin conjugates were targeted using nanobubbles under US effect. This system showed effective accumulation and cytotoxicity in HeLa cells. These nanobubbles also inhibited tumor in nude mice xenografted with HeLa cell tumors along with good body safety [115].

Conclusion

Ultrasound has shown its applicability in various fields including pharmaceutical advances in drug delivery and newer techniques for tracking drug carriers, triggering drug release, and enhancing drug deposition at the target with high precision using different nanocarriers like microbubbles, micelles, and liposomes. Further advancements in US-based triggered dislodgement of bioactive can bring newer horizons in nanotechnology-based strategies for therapeutic drug/gene targeting to tumors.

Compliance with ethical standards

Conflict of interest The authors declare that they have no conflict of interest.

References

1. Chowdhury SM, Lee T, Willmann JK. Ultrasound-guided drug delivery in cancer. Ultrasonography. 2017;36(3):171–84. 10.14366/usg.17021.
2. Suslick KS. Sonochemistry. Sonochem Sci. 1990;247(4949):1439–45. https://doi.org/10.1126/science.247.4949.1439.
3. Hill C, Bamber J. Methodology for clinical investigation. Phys Princ Med Ultrason 2004:255-85. https://doi.org/10.1002/0470093978.
4. Hynynen K. Macromolecular delivery across the blood–brain barrier. Macromol Drug Deliv Methods Protocol. 2009;480:175–85. https://doi.org/10.1007/978-1-59745-429-2_13.
5. Jernberg A. Ultrasound, ions and combined modalities for increased local tumour cell death in radiation therapy. Sweden: Institutionen för onkologi-patologi/Department of Oncology-Pathology; 2007.
6. Jain A, Jain SK. Liposomes in cancer therapy. Nanocarrier systems for drug delivery. Nova Science Publishers, https://www.novapublishers.com/catalog/product_info.php?products_id=59761&osCsid=e7d370318f328e75748328a1e44e48aa; 2016. p. 1–42.
7. Jain A, Jain S. Ligand-mediated drug-targeted liposomes. Liposomal delivery systems: advances and challenges. Future Medicine: UK; 2016. https://doi.org/10.4155/FSEB2013.14.251.
8. Saraf S, Jain A, Hurkat P, Jain SK. Topotecan liposomes: a visit from a molecular to a therapeutic platform. Crit Rev Ther Drug Carrier Syst. 2016;33(5):401–32. https://doi.org/10.1615/CritRevTherDrugCarrierSyst.2016015926.
9. Harvey EN, Harvey EB, Loomis AL. Further observations on the effect of high frequency sound waves on living matter. Biol Bull. 1928;55(6):459–69. https://doi.org/10.2307/1536801.
10. Lynn JG, Zwemer RL, Chick AJ, Miller AE. A new method for the generation and use of focused ultrasound in experimental biology. J Gen Physiol. 1942;26(2):179–93. https://doi.org/10.1085/jgp.26.2.179.
11. Goss S, Frizzell L, Dunn F. Ultrasonic absorption and attenuation in mammalian tissues. Ultrasound Med Biol. 1979;5(2):181–6. https://doi.org/10.1016/0301-5629(79)90086-3.
12. Lee C, Frizzell L. Exposure levels for ultrasonic cavitation in the mouse neonate. Ultrasound Med Biol. 1988;14(8):735–42. https://doi.org/10.1016/0301-5629(88)90029-4.
13. O'Brien WD, Simpson DG, Ho M-H, Miller RJ, Frizzell LA, Zachary JF. Superthreshold behavior and threshold estimation of ultrasound-induced lung hemorrhage in pigs: role of age dependency. IEEE Trans Ultrason Ferroelectr Freq Control. 2003;50(2):153–69. https://doi.org/10.1109/TUFFC.2003.1182119.
14. Billard B, Hynynen K, Roemer R. Effects of physical parameters on high temperature ultrasound hyperthermia. Ultrasound Med Biol. 1990;16(4):409–20. https://doi.org/10.1016/0301-5629(90)90070-S.
15. Daum DR, Smith NB, King R, Hynynen K. In vivo demonstration of noninvasive thermal surgery of the liver and kidney using an ultrasonic phased array. Ultrasound Med Biol. 1999;25(7):1087–98. https://doi.org/10.1016/S0301-5629(99)00053-8.
16. Damianou C, Hynynen K. The effect of various physical parameters on the size and shape of necrosed tissue volume during ultrasound surgery. J Acoust Soc Am. 1994;95(3):1641–9. https://doi.org/10.1121/1.408550.
17. Pichardo S, Sin VW, Hynynen K. Multi-frequency characterization of the speed of sound and attenuation coefficient for longitudinal transmission of freshly excised human skulls. Phys Med Biol. 2010;56(1):219–50. https://doi.org/10.1088/0031-9155/56/1/014.
18. Burtnyk M, N'Djin WA, Kobelevskiy I, Bronskill M, Chopra R. 3D conformal MRI-controlled transurethral ultrasound prostate therapy: validation of numerical simulations and demonstration in tissue-mimicking gel phantoms. Phys Med Biol. 2010;55(22):6817–39. https://doi.org/10.1088/0031-9155/55/22/014.
19. Pichardo S, Hynynen K. Treatment of near-skull brain tissue with a focused device using shear-mode conversion: a numerical study. Phys Med Biol. 2007;52(24):7313–32. https://doi.org/10.1088/0031-9155/52/24/008.
20. Pichardo S, Hynynen K. New design for an endoesophageal sector-based array for the treatment of atrial fibrillation: a parametric simulation study. IEEE Trans Ultrason Ferroelectr Freq Control. 2009;56(3):600–12. https://doi.org/10.1109/TUFFC.2009.1076.
21. Engel DJ, Muratore R, Hirata K, Otsuka R, Fujikura K, Sugioka K, et al. Myocardial lesion formation using high-intensity focused ultrasound. J Am Soc Echocardiogr. 2006;19(7):932–7. https://doi.org/10.1016/j.echo.2006.02.012.
22. Jin Z, Choi Y, Ko SY, Park JO, Park S. Experimental and simulation studies on focused ultrasound triggered drug delivery. Biotechnol Appl Biochem. 2017;64(1):134–42. https://doi.org/10.1002/bab.1453.
23. Leong T, Ashokkumar M, Kentish S. The fundamentals of power ultrasound—a review. Acoust Aust. 2011;39(2):54–63.
24. Hill C. The wider context of sonography. Phys Princ Med Ultrason. 2004:337–47.
25. Chavrier F, Chapelon J, Gelet A, Cathignol D. Modeling of high-intensity focused ultrasound-induced lesions in the presence of cavitation bubbles. J Acoust Soc Am. 2000;108(1):432–40. https://doi.org/10.1121/1.429476.
26. Sassaroli E, Hynynen K. Forced linear oscillations of microbubbles in blood capillaries. J Acoust Soc Am. 2004;115(6):3235–43. https://doi.org/10.1121/1.1738456.
27. Sokka S, Gauthier T, Hynynen K. Theoretical and experimental validation of a dual-frequency excitation method for spatial control of cavitation. Phys Med Biol. 2005;50(9):2167–79. https://doi.org/10.1088/0031-9155/50/9/017.
28. Aptel F, Lafon C. Therapeutic applications of ultrasound in ophthalmology. Int J Hyperth. 2012;28(4):405–18. https://doi.org/10.3109/02656736.2012.665566.
29. Zhou Y-F. High intensity focused ultrasound in clinical tumor ablation. World J Clin Oncol. 2011;2(1):8–27. https://doi.org/10.5306/wjco.v2.i1.8.
30. Melodelima D, N'Djin WA, Parmentier H, Chesnais S, Rivoire M, Chapelon J-Y. Thermal ablation by high-intensity-focused ultrasound using a toroid transducer increases the coagulated volume. Results of animal experiments. Ultrasound Med Biol. 2009;35(3):425–35. https://doi.org/10.1016/j.ultrasmedbio.2008.09.020.
31. Zhang K, Xu H, Jia X, Chen Y, Ma M, Sun L, et al. Ultrasound-triggered nitric oxide release platform based on energy transformation for targeted inhibition of pancreatic tumor. ACS Nano. 2016;10(12):10816–28. https://doi.org/10.1021/acsnano.6b04921.
32. Paparel P, Curiel L, Chesnais S, Ecochard R, Chapelon JY, Gelet A. Synergistic inhibitory effect of high-intensity focused ultrasound combined with chemotherapy on Dunning adenocarcinoma. BJU Int. 2005;95(6):881–5. https://doi.org/10.1111/j.1464-410X.2005.05420.x.

33. Tempany CM, Stewart EA, McDannold N, Quade BJ, Jolesz FA, Hynynen KMR. Imaging–guided focused ultrasound surgery of uterine leiomyomas: a feasibility study 1. Radiology. 2003;226(3):897–905. https://doi.org/10.1148/radiol.2271020395.
34. Harris GR, editor. FDA regulation of clinical high intensity focused ultrasound (HIFU) devices. Engineering in medicine and biology society, 2009. EMBC 2009. Annual International Conference of the IEEE; 2009: IEEE.
35. Grull H, Langereis S. Hyperthermia-triggered drug delivery from temperature-sensitive liposomes using MRI-guided high intensity focused ultrasound. J Control Release. 2012;161(2):317–27. https://doi.org/10.1016/j.jconrel.2012.04.041.
36. Güvener N, Appold L, de Lorenzi F, Golombek SK, Rizzo LY, Lammers T, et al. Recent advances in ultrasound-based diagnosis and therapy with micro-and nanometer-sized formulations. Methods (San Diego, Calif). 2017;130:4–13. https://doi.org/10.1016/j.ymeth.2017.05.018.
37. Husseini GA, Pitt WG. Ultrasonic-activated micellar drug delivery for cancer treatment. J Pharm Sci. 2009;98(3):795–811. https://doi.org/10.1002/jps.21444.
38. Mitragotri S. Healing sound: the use of ultrasound in drug delivery and other therapeutic applications. Nat Rev Drug Discov. 2005;4(3):255–60. https://doi.org/10.1038/nrd1662.
39. Escobar-Chavez JJ, Bonilla-Martínez D, Villegas-González MA, Rodríguez-Cruz IM, Domínguez-Delgado CL. The use of sonophoresis in the administration of drugs throughout the skin. J Pharm Pharm Sci. 2009;12(1):88–115. https://doi.org/10.18433/J3C30D.
40. Meijering BD, Juffermans LJ, van Wamel A, Henning RH, Zuhorn IS, Emmer M, et al. Ultrasound and microbubble-targeted delivery of macromolecules is regulated by induction of endocytosis and pore formation. Circ Res. 2009;104(5):679–87. https://doi.org/10.1161/CIRCRESAHA.108.183806.
41. Kedar RP, Cosgrove D, McCready VR, Bamber JC, Carter ER. Microbubble contrast agent for color Doppler US: effect on breast masses. Work in progress. Radiology. 1996;198(3):679–86. https://doi.org/10.1148/radiology.198.3.8628854.
42. Shin SH, Park E-J, Min C, Choi SI, Jeon S, Kim Y-H, et al. Tracking perfluorocarbon nanoemulsion delivery by 19F MRI for precise high intensity focused ultrasound tumor ablation. Theranostics. 2017;7(3):562–72. https://doi.org/10.7150/thno.16895.
43. Ries F, Honisch C, Lambertz M, Schlief R. A transpulmonary contrast medium enhances the transcranial Doppler signal in humans. Stroke. 1993;24(12):1903–9. https://doi.org/10.1161/01.STR.24.12.1903.
44. Wu J, Pepe J, Rincon M. Sonoporation, anti-cancer drug and antibody delivery using ultrasound. Ultrasonics. 2006;44:e21–e5. https://doi.org/10.1016/j.ultras.2006.06.033.
45. Togtema M, Pichardo S, Jackson R, Lambert PF, Curiel L, Zehbe I. Sonoporation delivery of monoclonal antibodies against human papillomavirus 16 E6 restores p53 expression in transformed cervical keratinocytes. PLoS One. 2012;7(11):e50730. https://doi.org/10.1371/journal.pone.0050730.
46. Liang H, Tang J, Halliwell M. Sonoporation, drug delivery, and gene therapy. Proc Inst Mech Eng H J Eng Med. 2010;224(2):343–61. https://doi.org/10.1243/09544119JEIM565.
47. Ferrante E, Pickard J, Rychak J, Klibanov A, Ley K. Dual targeting improves microbubble contrast agent adhesion to VCAM-1 and P-selectin under flow. J Control Release. 2009;140(2):100–7. https://doi.org/10.1016/j.jconrel.2009.08.001.
48. Treat LH, McDannold N, Vykhodtseva N, Zhang Y, Tam K, Hynynen K. Targeted delivery of doxorubicin to the rat brain at therapeutic levels using MRI-guided focused ultrasound. Int J Cancer. 2007;121(4):901–7. https://doi.org/10.1002/ijc.22732.
49. Jain A, Jain SK. Brain targeting using surface functionalized nanocarriers in human solid tumors. In: Singh B, Jain NK, Katare OP, editors. Drug nanocarriers, Series Nanobiomedicine, vol series ISBN: 1-62699-050-6. Houston LLC: Studium press; 2014. p. 203–55.
50. Jain A, Jain SK. Ligand-appended BBB-targeted Nanocarriers (LABTNs). Crit Rev Ther Drug Carrier Syst. 2015;32(2):149–80. https://doi.org/10.1615/CritRevTherDrugCarrierSyst.2015010903.
51. Hynynen K, McDannold N, Vykhodtseva N, Jolesz FA, Noninvasive MR. Imaging–guided focal opening of the blood-brain barrier in rabbits 1. Radiology. 2001;220(3):640–6. https://doi.org/10.1148/radiol.2202001804.
52. Sheikov N, McDannold N, Vykhodtseva N, Jolesz F, Hynynen K. Cellular mechanisms of the blood-brain barrier opening induced by ultrasound in presence of microbubbles. Ultrasound Med Biol. 2004;30(7):979–89. https://doi.org/10.1016/j.ultrasmedbio.2004.04.010.
53. Hynynen K, McDannold N, Sheikov NA, Jolesz FA, Vykhodtseva N. Local and reversible blood–brain barrier disruption by noninvasive focused ultrasound at frequencies suitable for trans-skull sonications. NeuroImage. 2005;24(1):12–20. https://doi.org/10.1016/j.neuroimage.2004.06.046.
54. Alonso A, Reinz E, Leuchs B, Kleinschmidt J, Fatar M, Geers B, et al. Focal delivery of AAV2/1-transgenes into the rat brain by localized ultrasound-induced BBB opening. Mol Ther-Nucleic Acids. 2013;2:e73.
55. Park J, Aryal M, Vykhodtseva N, Zhang Y-Z, McDannold N. Evaluation of permeability, doxorubicin delivery, and drug retention in a rat brain tumor model after ultrasound-induced blood-tumor barrier disruption. J Control Release. 2017;250:77–85. https://doi.org/10.1016/j.jconrel.2016.10.011.
56. Airan RD, Meyer RA, Ellens NP, Rhodes KR, Farahani K, Pomper MG, et al. Noninvasive targeted transcranial neuromodulation via focused ultrasound gated drug release from nanoemulsions. Nano Lett. 2017;17(2):652–9. https://doi.org/10.1021/acs.nanolett.6b03517.
57. Jain A, Jain SK. Stimuli-responsive smart liposomes in cancer targeting. Curr Drug Targets. 2016;17(11):1–11. https://doi.org/10.2174/1389450117666160208144143.
58. Jain A, Gulbake A, Jain A, Shilpi S, Hurkat P, Jain SK. Dual drug delivery using "smart" liposomes for triggered release of anticancer agents. J Nanopart Res. 2013;15(7):1–12.
59. Ta T, Porter TM. Thermosensitive liposomes for localized delivery and triggered release of chemotherapy. J Control Release. 2013;169(1–2):112–25. https://doi.org/10.1016/j.jconrel.2013.03.036.
60. Jain A, Jain SK. Multipronged, strategic delivery of paclitaxel-topotecan using engineered liposomes to ovarian cancer. Drug Dev Ind Pharm. 2016;42(1):136–49. https://doi.org/10.3109/03639045.2015.1036066.
61. Hynynen K, Lulu B. Hyperthermia in cancer treatment. Investig Radiol. 1990;25(7):824–34. https://doi.org/10.1097/00004424-199007000-00014.
62. Staruch RM, Ganguly M, Tannock IF, Hynynen K, Chopra R. Enhanced drug delivery in rabbit VX2 tumours using thermosensitive liposomes and MRI-controlled focused ultrasound hyperthermia. Int J Hyperthermia. 2012;28(8):776–87. https://doi.org/10.3109/02656736.2012.736670.
63. Li L, ten Hagen TL, Hossann M, Süss R, van Rhoon GC, Eggermont AM, et al. Mild hyperthermia triggered doxorubicin release from optimized stealth thermosensitive liposomes improves intratumoral drug delivery and efficacy. J Control Release. 2013;168(2):142–50. https://doi.org/10.1016/j.jconrel.2013.03.011.

64. Jain A, Jain SK. Colon targeted liposomal systems (CTLS): theranostic potential. Curr Mol Med. 2015;15(7):621–33. https://doi.org/10.2174/1566524015666150831131320.
65. Jain A, Jain SK. Environmentally responsive chitosan-based nanocarriers (CBNs). Handb Polym Pharm Technol Biodegrad Polym. 2015;3:105.
66. Jain A, Jain SK. Chapter 9: Application potential of engineered liposomes in tumor targeting. Multifunctional systems for combined delivery, biosensing and diagnostics. Elsevier - Health Sciences Division, https://www.elsevier.com/books/multifunctional-systems-for-combined-delivery-biosensing-and-diagnostics/grumezescu/978-0-323-52725-5; 2017. p. 171–92.
67. Ranjan A, Jacobs GC, Woods DL, Negussie AH, Partanen A, Yarmolenko PS, et al. Image-guided drug delivery with magnetic resonance guided high intensity focused ultrasound and temperature sensitive liposomes in a rabbit Vx2 tumor model. J Control Release. 2012;158(3):487–94. https://doi.org/10.1016/j.jconrel.2011.12.011.
68. Köhler MO, Mougenot C, Quesson B, Enholm J, Le Bail B, Laurent C, et al. Volumetric HIFU ablation under 3D guidance of rapid MRI thermometry. Med Phys. 2009;36(8):3521–35. https://doi.org/10.1118/1.3152112.
69. Hijnen N, Kneepkens E, de Smet M, Langereis S, Heijman E, Grüll H. Thermal combination therapies for local drug delivery by magnetic resonance-guided high-intensity focused ultrasound. Proc Natl Acad Sci. 2017:201700790.
70. Dai M, Wu C, Fang H-M, Li L, Yan J-B, Zeng D-L et al. Thermo-responsive magnetic liposomes for hyperthermia-triggered local drug delivery. J Microencapsul. 2017(just-accepted):1–18.
71. Jang KW, Seol D, Ding L, Heo DN, Lee SJ, Martin JA, et al. Ultrasound-triggered PLGA microparticle destruction and degradation for controlled delivery of local cytotoxicity and drug release. Int J Biol Macromol. 2017; https://doi.org/10.1016/j.ijbiomac.2017.08.125.
72. Boissenot T, Bordat A, Larrat B, Varna M, Chacun H, Paci A, et al. Ultrasound-induced mild hyperthermia improves the anticancer efficacy of both Taxol® and paclitaxel-loaded nanocapsules. J Control Release. 2017;264:219–27. https://doi.org/10.1016/j.jconrel.2017.08.041.
73. Feng G, Hao L, Xu C, Ran H, Zheng Y, Li P, et al. High-intensity focused ultrasound-triggered nanoscale bubble-generating liposomes for efficient and safe tumor ablation under photoacoustic imaging monitoring. Int J Nanomedicine. 2017;12:4647–59. https://doi.org/10.2147/IJN.S135391.
74. Zhang N, Li J, Hou R, Zhang J, Wang P, Liu X, et al. Bubble-generating nano-lipid carriers for ultrasound/CT imaging-guided efficient tumor therapy. Int J Pharm. 2017;534(1-2):251–62. https://doi.org/10.1016/j.ijpharm.2017.07.081.
75. Santos MA, Goertz DE, Hynynen K. Focused ultrasound hyperthermia mediated drug delivery using thermosensitive liposomes and visualized with in vivo two-photon microscopy. Theranostics. 2017;7(10):2718–31. https://doi.org/10.7150/thno.19662.
76. Umemura S, Yumita N, Nishigaki R, Umemura K. Mechanism of cell damage by ultrasound in combination with hematoporphyrin. Cancer Sci. 1990;81(9):962–6.
77. Trendowski M. The promise of sonodynamic therapy. Cancer Metastasis Rev. 2014;33(1):143–60. https://doi.org/10.1007/s10555-013-9461-5.
78. Chen H, Zhou X, Gao Y, Zheng B, Tang F, Huang J. Recent progress in development of new sonosensitizers for sonodynamic cancer therapy. Drug Discov Today. 2014;19(4):502–9. https://doi.org/10.1016/j.drudis.2014.01.010.
79. Costley D, Mc Ewan C, Fowley C, McHale AP, Atchison J, Nomikou N, et al. Treating cancer with sonodynamic therapy: a review. Int J Hyperth. 2015;31(2):107–17. https://doi.org/10.3109/02656736.2014.992484.
80. Liu Q, Wang X, Wang P, Xiao L, Hao Q. Comparison between sonodynamic effect with protoporphyrin IX and hematoporphyrin on sarcoma 180. Cancer Chemother Pharmacol. 2007;60(5):671–80. https://doi.org/10.1007/s00280-006-0413-4.
81. Zhu B, Liu Q, Wang Y, Wang X, Wang P, Zhang L, et al. Comparison of accumulation, subcellular location, and sonodynamic cytotoxicity between hematoporphyrin and protoporphyrin IX in L1210 cells. Chemotherapy. 2010;56(5):403–10. https://doi.org/10.1159/000317743.
82. Sugita N, Iwase Y, Yumita N, Ikeda T, Umemura S-I. Sonodynamically induced cell damage using rose bengal derivative. Anticancer Res. 2010;30(9):3361–6.
83. Chen M, Xu A, He W, Ma W, Shen S. Ultrasound triggered drug delivery for mitochondria targeted sonodynamic therapy. J Drug Deliv Sci Technol. 2017;39:501–7. https://doi.org/10.1016/j.jddst.2017.05.009.
84. Suzuki N, Okada K, Chida S, Komori C, Shimada Y, Suzuki T. Antitumor effect of acridine orange under ultrasonic irradiation in vitro. Anticancer Res. 2007;27(6B):4179–84.
85. Z-Y X, Wang K, Li X-Q, Chen S, Deng J-M, Cheng Y, et al. The ABCG2 transporter is a key molecular determinant of the efficacy of sonodynamic therapy with Photofrin in glioma stem-like cells. Ultrasonics. 2013;53(1):232–8.
86. Hiraoka W, Honda H, Feril LB, Kudo N, Kondo T. Comparison between sonodynamic effect and photodynamic effect with photosensitizers on free radical formation and cell killing. Ultrason Sonochem. 2006;13(6):535–42. https://doi.org/10.1016/j.ultsonch.2005.10.001.
87. Stępniewski M, Kepczynski M, Jamróz D, Nowakowska M, Rissanen S, Vattulainen I, et al. Interaction of hematoporphyrin with lipid membranes. J Phys Chem B. 2012;116(16):4889–97. https://doi.org/10.1021/jp300899b.
88. Tang W, Liu Q, Wang X, Mi N, Wang P, Zhang J. Membrane fluidity altering and enzyme inactivating in sarcoma 180 cells post the exposure to sonoactivated hematoporphyrin in vitro. Ultrasonics. 2008;48(1):66–73. https://doi.org/10.1016/j.ultras.2007.10.002.
89. Qian X, Zheng Y, Chen Y. Micro/nanoparticle-augmented sonodynamic therapy (SDT): breaking the depth shallow of photoactivation. Advanced materials (Deerfield Beach, Fla). 2016;28(37):8097–129. https://doi.org/10.1002/adma.201602012.
90. Kujawska T, Secomski W, Bilmin K, Nowicki A, Grieb P. Impact of thermal effects induced by ultrasound on viability of rat C6 glioma cells. Ultrasonics. 2014;54(5):1366–72. https://doi.org/10.1016/j.ultras.2014.02.002.
91. Li L, Chen Y, Wang X, Feng X, Wang P, Liu Q. Comparison of protoporphyrin IX produced cell proliferation inhibition between human breast cancer MCF-7 and MDA-MB-231 cells. Die Pharm—Int J Pharm Sci. 2014;69(8):621–8.
92. Guo S, Sun X, Cheng J, Xu H, Dan J, Shen J, et al. Apoptosis of THP-1 macrophages induced by protoporphyrin IX-mediated sonodynamic therapy. Int J Nanomedicine. 2013;8:2239–46. https://doi.org/10.2147/IJN.S43717.
93. Serpe L, Giuntini F. Sonodynamic antimicrobial chemotherapy: first steps towards a sound approach for microbe inactivation. J Photochem Photobiol B Biol. 2015;150:44–9. https://doi.org/10.1016/j.jphotobiol.2015.05.012.
94. Zhang H, Liu X, Liu Y, Wu Y, Li H, Zhao C, et al. Effect of hematoporphyrin monomethyl ether-sonodynamic therapy (HMME-SDT) on hypertrophic scarring. PLoS One. 2014;9(1):e86003. https://doi.org/10.1371/journal.pone.0086003.
95. Machet L, Boucaud A. Phonophoresis: efficiency, mechanisms and skin tolerance. Int J Pharm. 2002;243(1):1–15. https://doi.org/10.1016/S0378-5173(02)00299-5.

96. Samulski T, Grant W, Oleson J, Leopold K, Dewhirst M, Vallario P, et al. Clinical experience with a multi-element ultrasonic hyperthermia system: analysis of treatment temperatures. Int J Hyperth. 1990;6(5):909–22. https://doi.org/10.3109/02656739009140972.
97. Klingler HC, Susani M, Seip R, Mauermann J, Sanghvi N, Marberger MJ. A novel approach to energy ablative therapy of small renal tumours: laparoscopic high-intensity focused ultrasound. Eur Urol. 2008;53(4):810–8. https://doi.org/10.1016/j.eururo.2007.11.020.
98. McAteer J, Bailey M, Williams JJ, Cleveland R, Evan A. Strategies for improved shock wave lithotripsy. Minerva Urol Nefrol= Ital J Urol Nephrol. 2005;57(4):271–87.
99. Koga H, Matsuoka K, Noda S, Yamashita T. Cumulative renal damage in dogs by repeated treatment with extracorporeal shock waves. Int J Urol. 1996;3(2):134–40. https://doi.org/10.1111/j.1442-2042.1996.tb00498.x.
100. Kim SC, Matlaga BR, Tinmouth WW, Kuo RL, Evan AP, McAteer JA, et al. In vitro assessment of a novel dual probe ultrasonic intracorporeal lithotriptor. J Urol. 2007;177(4):1363–5. https://doi.org/10.1016/j.juro.2006.11.033.
101. Lowe G, Knudsen BE. Ultrasonic, pneumatic and combination intracorporeal lithotripsy for percutaneous nephrolithotomy. J Endourol. 2009;23(10):1663–8. https://doi.org/10.1089/end.2009.1533.
102. Packer M, Fishkind WJ, Fine IH, Seibel BS, Hoffman RS. The physics of phaco: a review. J Cataract Refract Surg. 2005;31(2):424–31. https://doi.org/10.1016/j.jcrs.2004.11.027.
103. Parikh S, Motarjeme A, McNamara T, Raabe R, Hagspiel K, Benenati JF, et al. Ultrasound-accelerated thrombolysis for the treatment of deep vein thrombosis: initial clinical experience. J Vasc Interv Radiol. 2008;19(4):521–8. https://doi.org/10.1016/j.jvir.2007.11.023.
104. Farinha A, Kellogg S, Dickinson K, Davison T. Skin impedance reduction for electrophysiology measurements using ultrasonic skin permeation: initial report and comparison to current methods. Biomed Instrum Technol. 2006;40(1):72–7. https://doi.org/10.2345/0899-8205(2006)40[72:SIRFEM]2.0.CO;2.
105. Gebauer D, Mayr E, Orthner E, Ryaby JP. Low-intensity pulsed ultrasound: effects on nonunions. Ultrasound Med Biol. 2005;31(10):1391–402. https://doi.org/10.1016/j.ultrasmedbio.2005.06.002.
106. Tung CH, Han MS, Kim Y, Qi J, O'Neill BE. Tumor ablation using low-intensity ultrasound and sound excitable drug. J Controlled release : Off J Control Release Soc. 2017;258:67–72. https://doi.org/10.1016/j.jconrel.2017.05.009.
107. Staruch R, Chopra R, Hynynen K. Localised drug release using MRI-controlled focused ultrasound hyperthermia. Int J Hyperth. 2011;27(2):156–71. https://doi.org/10.3109/02656736.2010.518198.
108. Kong G, Anyarambhatla G, Petros WP, Braun RD, Colvin OM, Needham D, et al. Efficacy of liposomes and hyperthermia in a human tumor xenograft model: importance of triggered drug release. Cancer Res. 2000;60(24):6950–7.
109. Jain A, Jain SK. In vitro release kinetics model fitting of liposomes: an insight. Chem Phys Lipids. 2016;201:28–40. https://doi.org/10.1016/j.chemphyslip.2016.10.005.
110. Matsumura Y, Maeda H. A new concept for macromolecular therapeutics in cancer chemotherapy: mechanism of tumoritropic accumulation of proteins and the antitumor agent smancs. Cancer Res. 1986;46(12 Pt 1):6387–92.
111. White SC, Lorigan P, Margison GP, Margison JM, Martin F, Thatcher N, et al. Phase II study of SPI-77 (sterically stabilised liposomal cisplatin) in advanced non-small-cell lung cancer. Br J Cancer. 2006;95(7):822–8. https://doi.org/10.1038/sj.bjc.6603345.
112. Yudina A, Lepetit-Coiffé M, De Smet M, Langereis S, Grüll H, Moonen C. Vivo temperature controlled ultrasound-mediated intracellular delivery of cell-impermeable compounds. J Control Release. 2012;161(1):90–7. https://doi.org/10.1016/j.jconrel.2012.04.018.
113. Min HS, Son S, You DG, Lee TW, Lee J, Lee S, et al. Chemical gas-generating nanoparticles for tumor-targeted ultrasound imaging and ultrasound-triggered drug delivery. Biomaterials. 2016;108:57–70. https://doi.org/10.1016/j.biomaterials.2016.08.049.
114. Lin W, Xie X, Deng J, Liu H, Chen Y, Fu X, et al. Cell-penetrating peptide-doxorubicin conjugate loaded NGR-modified nanobubbles for ultrasound triggered drug delivery. J Drug Target. 2016;24(2):134–46. https://doi.org/10.3109/1061186X.2015.1058802.
115. Xie X, Lin W, Liu H, Deng J, Chen Y, Liu H, et al. Ultrasound-responsive nanobubbles contained with peptide–camptothecin conjugates for targeted drug delivery. Drug Deliv. 2016;23(8):2756–64. https://doi.org/10.3109/10717544.2015.1077289.